IEEE Access
Multidisciplinary | Rapid Review | Open Access Journal

Received 29 January 2023, accepted 22 February 2023, date of publication 2 March 2023, date of current version 16 March 2023.

Digital Object Identifier 10.1109/ACCESS.2023.3251356

RESEARCH ARTICLE

Operation Strategy of EV Aggregators Considering EV Driving Model and Distribution System Operation in Integrated Power and Transportation Systems

HEEJUNE CHA[1], MYEONGSEOK CHAE[2], (Student Member, IEEE), MUHAMMAD AHSAN ZAMEE[2], AND DONGJUN WON[2], (Member, IEEE)

[1]Airport Industry Technology Research Institute, Incheon International Airport Corporation (IIAC), Incheon 22382, South Korea
[2]Department of Electrical and Computer Engineering, Inha University, Incheon 22212, South Korea

Corresponding author: Dongjun Won (djwon@inha.ac.kr)

This work was supported by Inha University Research Grant.

ABSTRACT Recently, the penetration of electric vehicle (EV) has increased, and several motor companies have declared a paradigm shift to EVs. However, most existing studies focusing on EV charging scheduling in power system operations neglect the integrated operation of transportation and distribution systems. Because EVs affect both systems, it is necessary to consider the grid operation and the individual EV's preferences (charging cost and time) simultaneously. In this study, an integrated power-transportation system structure and operation algorithms are developed to analyze the impact of EVs on the distribution system. In addition, this study proposes an optimal EV driving model that consists of two driving patterns: routine driving and long-distance driving. For routine driving patterns, the Markov chain model is implemented considering the mileage and conditions of individual EVs. Subsequently, long-distance driving patterns are developed to select the optimal route through reinforcement learning. In addition, the EV aggregator structure of EV charging stations can effectively predict local charge demands and perform charge control in real-time. An integrated power-transportation system is developed using the IEEE RBTS system and the integrated system architecture and algorithms are developed using MATLAB. It utilizes the ACOPPF function of MATPOWER to evaluate systematic stability and derive DLMP (Distributed Locational Marginal Price). This study conducts performance verification in various scenarios, confirming the effect of charging control of EV aggregators considering system stability, loss reduction, and cost reduction of the entire system.

INDEX TERMS Electric vehicle, route selection, aggregator, power-transportation system, driving scheduling, charging scheduling.

NOMENCLATURE

p^t	*The probability of change at time t-1.*
SOC_ϵ	*The initial State-of-charge.*
s_{num}	*The state count by MDP environment.*
i, j	*The starting/arrival point.*
$EV_{perform}$	*The drive performance of EVs (kWh/km).*
d_{ij}	*The distance from i to j.*
$Price_{ch}(j)$	*The charging rate at location j.*
$t_{depa}(j)$	*The Arrival time from departure point to j.*
t_{req}	*The charging time.*
P_{fast}	*The power output of quick charge.*

The associate editor coordinating the review of this manuscript and approving it for publication was Chenghong Gu.

$x_i(t)$	*The charging station schedule by adjusted time.*
$x_j(t)$	*The general load for the entire system by adjusted time.*
AG	*The number of charging stations in the system.*
T	*The simulation time.*
$P_i^{sch}(t)$	*The submitted charging station schedule via time.*
$Load_j(t)$	*The general load for the entire system via time.*

I. INTRODUCTION

Recently, EVs have attracted attention because of their eco-friendliness, considering issues such as the increase in greenhouse gases caused by internal combustion engine vehicles and global warming [1]. In addition to current policies for supplying EVs by countries, it is expected to achieve a 30% penetration rate of EVs [2]. An increase in the supply of EVs can significantly impact the power system, and a system for smart grid technology and stable system operation is required to stabilize the power supply and demand [3].

EVs have had problems with long-term charging times in the early days and problems with range anxiety due to their battery capacity; however, several efforts have been made to develop technologies to solve them. Because of the development of technology for EVs, BEVs (Battery EVs) such as Tesla's Model S and Chevrolet's Volt also has a mileage of more than 400 km, and sales of such BEVs are on the increase globally [3], [4], [5]. While such high-capacity fast charging technology and improved battery performance led to significant progress in driving EVs, the impact on the power system has become more critical [6], [7]. The effects of EVs on the system can cause problems such as increased power transmission losses in the system, increased load peaks, voltage problems in the distribution system, premature aging of the transformer, overloading the transmission capacity, system reconfiguration, and infrastructure expansion [6], [7], [8], [9].

Research that considers EVs can be divided into two main types when operating the system. First, EVs are scheduled from the perspective of a system operator, such as a distribution system operator (DSO) or microgrid operator (MGO). Therefore, these studies mainly used stochastic charging time to reflect the characteristics of EVs in the general optimal system operation method. Second, EVs usually only treat EVs as loads or ESS and use them for system operation, so there may be some parts that need to consider the actual selectable rational behavior of EV drivers. An example is participation in control or frequency adjustment services inhibiting variability in renewable energy. Reference [10] and [11] contributed to the grid by utilizing it for frequency adjustment and renewable energy output assistance, respectively, through several EVs, but the driver's behavior is not being considered, making it any different from ESS.

To solve the above problem, there are studies that introduced EV aggregators. This EV aggregator refers to middle managers, such as parking lots and charging stations, and considers individual benefits from two perspectives through the hierarchical structure. As system operators cannot monitor or control individual EVs, they have a structure that communicates with multiple EVs through EV aggregators to control charging and discharging.

EV aggregator participation in the EV power market (capacity market, reserve ancillary service like reserve market, frequency regulation, others) is typical, and as shown in [12], system operators pass key variables of system constraints to EV aggregators, which have a hierarchical structure of charging individual EVs. In addition to driving patterns, there are studies that show that charging patterns change in consideration of EV drivers' propensity [13]. However, this paper did not consider changes in driving patterns and charging positions.

It is common that consider the drivability of EVs, selecting the optimal charging location and path. These studies mainly establish a transportation system to select the optimal route from a particular origin to a destination and determines the route of public transportation such as buses and taxis. However, considering the time and region charging rates only, the drivability of EVs is similar to load shifting in the power system. This problem can cause the power system in the power market, where local differential rates such as locational margin prices (LMPs). For this reason, [4] induced congestion to be mitigated by fluctuating charging rates in consideration of power system congestion and voltage stability. A previous study [14] changed the LMP at the location at the time the vehicle is charged, leading the next vehicle to a lower price; however, there is a limitation that the distance between nodes does not reflect the charging rate and the vehicle's driving path in real-time.

There is also a study on the distribution-LMP calculation that applies the concept of LMP to the distribution system for stable operation. [15] conducted a study on the calculation of DLMP by considering EVs, OLTCs (On Load Tap Changer), and reconfiguration of feeders. Reference [16] calculated the DLMP based on the day-ahead LMP and the expected load and used it for power system operation by considering the system congestion through the expected charge of EVs. However, neither study considered variability in real-time nor based it solely on scheduling. If the DLMP calculated based on the day-ahead scheduling increases, the vehicle could make different choices on the actual operation day. In this study, we focused on distributing EVs through local pricing considering power system stability. In contrast [17] focused on EV drivers so that they could choose optimal routing between multiple EVs as a way of considering EV drivers' minimum latency, driving time, and charge. Reference [18] conducted an iterative least cost vehicle routing process that utilizes the communication of EVs with competing charging

stations to exchange data such as electricity price, energy demand, and arrival time. [19] focused on determining the optimal number of EV charging stations to install. However, both studies did not consider system stability and cost reduction of the entire system. Reference [20] shows the optimal scheduling of V2G, [21], [22] showed the integrated power-transportation system structure modeling. Reference [23] proposed the charging scheduling problem of a park-and-charge system considering the EV battery charging degradation cost while satisfying the battery charging characteristic. Reference [24] showed the battery degradation cost model of EV lithium-ion batteries with the optimal charging schedule of 400 EVs.

Still, these papers only showed the optimal operation in emergencies and did not focus on the information required for the actual operating system and the system's stable operation.

The contributions of this paper are listed as follows:

1. Integrated power-transportation system structure modeling: Driving schedule modeling of EVs using the Markov chain model and structural modeling of power-transportation systems.

In the integrated system, an operation algorithm that considers both the traffic-centric and electric power-centric views of EVs was presented, and a more realistic situation was simulated.

2. Development of EV aggregator's day-ahead charging scheduling and real-time charging algorithm: Development of EV aggregator's algorithm for EV aggregators considering vehicle driving schedule, parking time, and required energy. Furthermore, by presenting the coordination algorithm between EV aggregators, it is possible to solve the problem that occurs at a single charging station.

3. Development of an optimal charging and driving path selection algorithm for vehicles using reinforcement learning: Development of an optimal charging and driving path selection algorithm considering DLMP based on reinforcement learning. DLMP contributes to solving the instantaneous peak and local voltage problems in the LMP market.

As a result, the effect of EV charging on the distribution system was analyzed, and the operation of the EV aggregator can contribute to the system's stable operation. In addition, the effect of charging cost on vehicle route selection has been confirmed, and the power system can distribute charging demand through DLMP.

In this study, the effects of EV aggregators on distribution systems with increasing distribution of EVs and changes in power system structure in distributed energy are studied.

Section II describes the structure of the entire system and Section III deals with the individual modeling of EVs and the operational algorithm of EV aggregators.

In Section IV, the results are analyzed by performing a case study of the proposed structure. Section V presents the conclusions of the study and directions for future research. The main points of this paper are 1) analysis of the systematic operation impact of EV charging in the integrated deployment environment of transportation and power systems, 2) the operation algorithm of the EV aggregators, and 3) changes in the EV driving path and system impact considering the regional differential price.

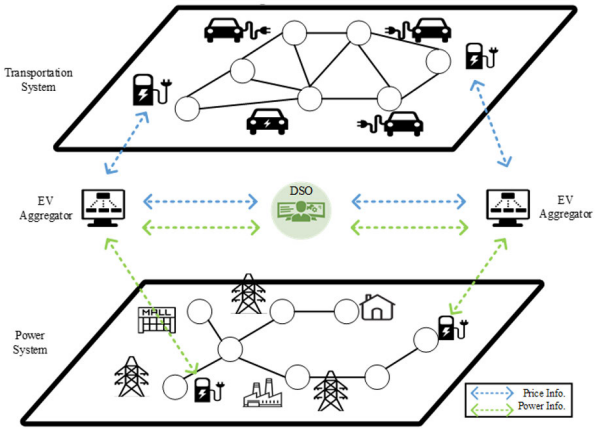

FIGURE 1. Integrated system structure.

II. DESIGN OF THE INTEGRATED SYSTEM

A. CONCEPT OF INTEGRATED SYSTEMS

EVs can be a distributed energy source close to consumers at home. However, as individual EVs participate in the electricity market, the capacity is small to monitor and control the distribution system operator (DSO), which is a burden for system operators to communicate with all EVs. In addition, controlling this individually requires considerable data from DSOs, and it is difficult to operate while satisfying the driver's needs.

Figure 1 shows a general structure that enables system operations and EV market participation in conjunction with DSOs, with EV aggregators to manage EVs [17], [24]. In this structure, EV drivers can check system prices and charge at low prices, and DSOs can use EV aggregators to identify and use the power consumed in charging EVs without managing individual EVs. EV aggregators manage multiple charging stations (EVCSs) in each region, each managing charging EVs in the neighboring region. The EV aggregator is typically located between the DSO and the EV driver in the power system. In addition, EV aggregators can predict charging schedules by receiving information such as driving schedules or charging demand times from EVs.

Figure 2 shows the architecture of the integrated power-transportation system. The higher layer is the grid of the traffic system, and the lower layer is the power distribution system simulated by the IEEE RBTS system. In this figure, the blue area is residential, the red area is commercial, and the orange areas have high loads of factory characteristics; the light green area was divided into areas with charging stations and areas for charging EVs. An EV charging load is connected to a single node, which is connected through a particular link when charging an EV in a nearby area. Moreover, it is assumed that all EVs connected to the corresponding nodes can be communicated with EV aggregators

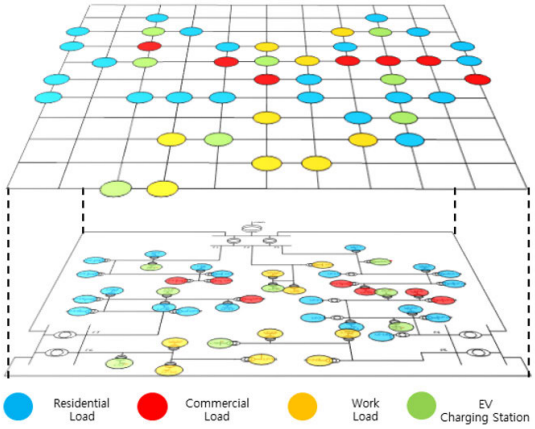

FIGURE 2. Integrated power-transportation system structure.

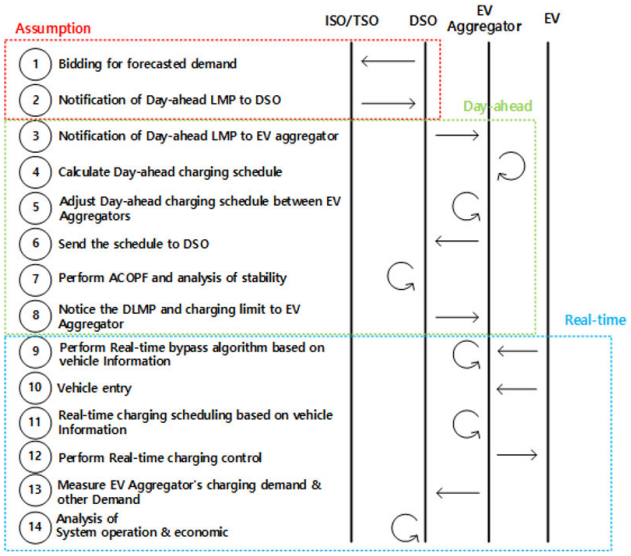

FIGURE 3. Operating scheme for integrated systems.

about charging control and data collection system. Several EV operations occur in transportation systems, and the link managed by EV aggregators reflects the charging power of parked EVs.

Therefore, the power system performs system operation based on the load usage of the corresponding node. EVs' driving pattern also affects the DLMP calculations during the day-ahead. It is also assumed that these calculated DLMPs affect the EV driving schedule again, resulting in the interaction between the two systems.

Figure 3 shows the overall operational scheme of the proposed system. Figures 1 and 2 assume demand bids and pricing between market operators and DSOs have ended. As discussed earlier, this paper only deals with the problem at the transmission level by studying the distribution systems. Moreover, it is assumed that it has already been performed for the LMP calculation process at the transmission level. Therefore, the DSO's demand bidding and LMP determination process is not addressed, and DSO utilizes LMP to operate the distribution system. (① -②)

Aftermarket clearing in the transmission system, the DSO informs the EV aggregator of the LMP determined on the day-ahead (③). It predicts the EV parking schedule expected to be entered the next day for each charging station. It calculates the charging schedule by considering the LMP received from the EV aggregator (④). The EV aggregator receives charging scheduling results of the day-ahead from the charging stations located by region.

The EV aggregator adjusts the charging schedule between charging stations based on the day-ahead charging schedule results for several charging stations (⑤). The EV aggregator delivers the adjusted charging scheduling results to the DSO (⑥). The DSO performs ACOPF (AC Optimal Power Flow) for all time of the following day, reflecting the EV's charging schedule with the expected general load (⑦).

The DSO provides the charging limit capacity of the charging station along with the DLMP obtained during the system analysis if there is no problem with the system operation after the system analysis (⑧). ③-⑧ is the day-ahead operation section and is reflected in the EV charging control of the EV aggregator and operation of the day-ahead power system.

On the same day, real-time system operation is simulated in a 15 min time step. The EV aggregator receives driving and charging information from EVs only for vehicles selecting the optimal route, updates the price information based on the real-time charging station situation, and delivers it to EVs. EVs perform optimal route selection based on the updated pricing (⑨). The EV checks the parking conditions according to the driving schedule by time periods (⑩). Each charging station conducts a charging schedule for a parked vehicle (⑪). It performs charge control within the charging capacity according to priority. After charging the EV, the DSO calculates power flow to check the system condition (⑫-⑬). As a result of calculating DLMP and the day-ahead schedule management results, stable impact and economic feasibility are analyzed from the system perspective on results after the real-time operation (⑭).

III. SCHEDULING & OPERATION ALGORITHM OF EV AGGREGATORS

Section III describes how to model the driving schedule for EVs and EV aggregators. As mentioned in Section II, the driving schedule for EVs is divided into two types: routine driving and long-distance driving. The EV driving schedule model for routine driving is when the charging position does not change with routine driving, but the charging time changes with the price.

In the case of long-distance driving, on the contrary, it determines which route and where to charge for long-distance. Furthermore, this section shows the EV aggregator's operational algorithm for charging scheduling and control individual EVs.

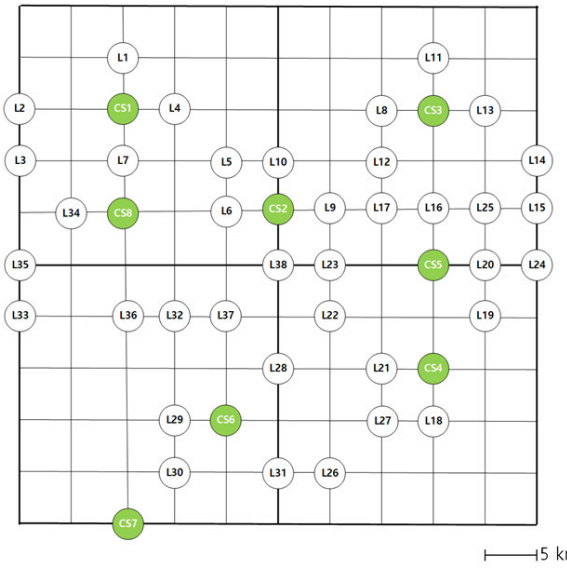

FIGURE 4. Transportation system structure in target area.

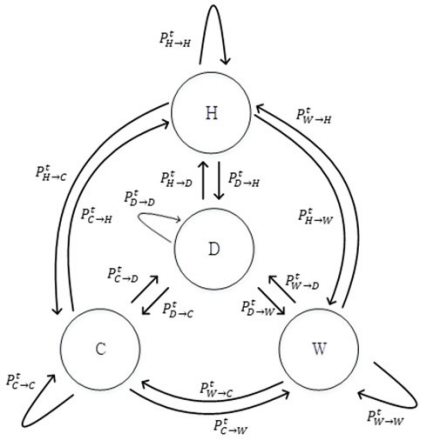

FIGURE 5. Markov chain diagram.

A. EV SCHEDULING MODEL

Figure 4 shows the power system of the integrated system onto the transportation system for routine driving schedules. The distance between the lattices is 5 km, and 1 step is assumed to be moved during 1 time step, defined as 15 min. For EV charging, the green-marked part in Figure 4 becomes the charging station (CS) that performs charging, assuming it is connected through a track. Each CS is responsible for managing the charging of EVs connected to the surrounding loads, which are buses that meet the charging needs of the surrounding area for the convenience of research but are assumed to be one CS on the system. Therefore, there is assumed to be vehicle movement between CS and CS in Figure 4.

Before considering the power system, a Markov chain model was developed to derive the mileage and driving conditions of EVs by referring to the study in [25]. It also obtained and applied vehicle data by referring to the 2017 travel data from the National Home Travel Survey (NHTS). [26]

Figure 5 shows a Markov chain diagram showing the state change in EV at t - *1* time to EV at time t.

In this figure, the abbreviations have the following meanings: the state drive (D) – residential (H) – working (W) – commercial (C), and P will be described in Equation (1). The figure shows the next time of each state and the probability of each state. In probability, the probability of changing from driving to the home state at t - *1* time is expressed as $P^t_{D\to H}$. Equation (1) is a modification of the Markov chain diagram shown in Figure 5, and an hourly Markov chain matrix representing the probability of changing from time t - 1 to time t state. For all simulation times, such a Markov chain model was applied to determine the state of each time step to generate the one-day driving data of one EV.

Subsequently, the travel distance between state changes is calculated from the time period-specific state data obtained from the driving data, and the location in Figure 4 is synchronized as much as possible. In this study, the driving time between the state data is calculated to derive the location data from the driving state data. Each vehicle calculates a travelable distance according to the driving time from a position arbitrarily determined by its initial state to determine its post-driving position. The initial SOC of the battery is set to be determined by the gamma distribution, as shown in (2) and (3):

$$T_t = \begin{bmatrix} P^t_{D\to D} & P^t_{D\to H} & P^t_{D\to W} & P^t_{D\to C} \\ P^t_{H\to D} & P^t_{H\to H} & P^t_{H\to W} & P^t_{H\to Q} \\ P^t_{W\to D} & P^t_{W\to H} & P^t_{W\to W} & P^t_{W\to C} \\ P^t_{C\to D} & P^t_{C\to H} & P^t_{C\to W} & P^t_{C\to C} \end{bmatrix} \tag{1}$$

$$y = f\,(x|\,a,b) = \frac{1}{b^a\Gamma\,(a)} x^{a-1} e^{\frac{-x}{b}} \tag{2}$$

$$SOC_\epsilon = 15 + y \tag{3}$$

where a is the shape parameter, b is the scale parameter and SOC_ϵ is initial SOC.

B. DRIVING SCHEDULING OF LONG-DISTANCE VEHICLES WITH REINFORCEMENT LEARNING

Unlike in Figure 4, within the target area, long-distance driving vehicles perform their schedules in the traffic system structure in Figure 6. Given the long-distance driving, Figure 4 shows the distance between grids set to 5 km, and Figure 6 sets it to 15 km. As previously discussed, we derive the driving schedule by selecting the optimal charging and driving path using RL. In addition, a route can be moved from the origin to the destination to simplify the simulation.

As shown in Figure 6, the state is limited to the origin-destination and charging area. The action is limited to the driving route to another state and charging after driving the origin route. For example, the action available at the origin is CS 3; if not CS 3, the following available charging locations are CSs 1 or 5.

Figure 7 shows a flowchart of the route selection algorithm. First, the EV drive schedule calculates the required charging

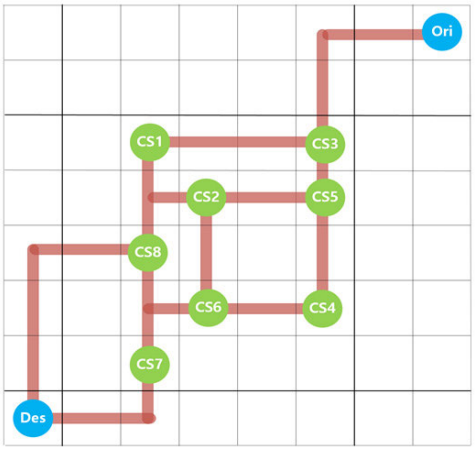

FIGURE 6. Transportation system structure of long-distance vehicles.

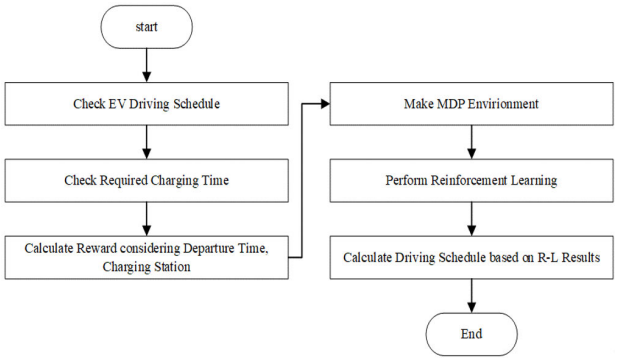

FIGURE 7. Flowchart of driving route selection algorithm using reinforcement learning.

capacity that must be charged, and the charging time required for fast charging is inversely calculated. Subsequently, the charging cost for each CS and the amount of electricity consumed in the moving route according to the departure time of the origin are applied as reinforcement learning to calculate the moving route and charging route. Then, the MDP is composed of the state of the point, the action indicating the route or charging state, and the cost meaning the reward. Finally, a vehicle driving and charging schedule are calculated based on the derived results.

Equation (4), as shown at the bottom of the page, is a state set for the state in each environment, (5), as shown at the bottom of the page, is an action set with a total of four actions, divided into two driving paths and charging behavior after driving, where s_{num} is state count by MDP environment. Furthermore, because reinforcement learning typically learns to maximize rewards, this work consists of rewards considering the minimum charging cost and distance (cost to the amount of electricity consumed while driving).

Suppose the typical driving behavior is chosen in (6), as shown at the bottom of the page. In that case, the compensation value is calculated as the cost of consumption energy according to the mileage, where i is the starting point, j is the arrival point, $Price$ is the charging rate (LMP or DLMP), $EV_{perform}$ is the drive performance of EVs (kWh/km). d_{ij} is the distance from i to j, $Price_{ch}(j)$ is the charging rate when charging at location j. The electricity bill is applied to average of price, which is to be converted into an expense, assuming that the vehicle has been charged at an average rate on the same day because it doesn't know the cost of charging previously. Assuming that the EV is charged at an average rate, the power consumption for the distance traveled along the route can be converted into a cost. The calculation for the second term is when the cost of driving distance calculated earlier considers the cost of charging at that location. If the destination simply moved from the destination to CS3, the cost for the distance traveled is regarded as -reward as it corresponds to the first term in Equation (6). On the other hand, if charging is performed after moving to CS3, it is considered a -reward considering the cost of moving distance and charging cost. If all four actions do not exist, move to any state that is not connected,

leaving the reward as $-\infty$ to disable it.

Equation (7), as shown at the bottom of the page, calculates the charging cost at the destination point in such cases, where $t_{depa}(j)$ is arrival time from starting point to j, t_{req} is charging time, P_{fast} is quick charging output. In Figure 6, for charging in CS2, the arrival time is specified regardless of the driving path. This is because the transportation system is lattice-structured, going to the destination located diagonally, and if CS2 does not charge, it does not charge anywhere else but only driving. In other words, arriving at CS 2 at the seventh time step after departure from the origin does not

$$S = \{s_1, s_2, \ldots, s_{num}\} \tag{4}$$

$$A = \{a_{r1}, a_{cr1}, a_{r2}, a_{cr2}\} \tag{5}$$

$$r_i(a_i) = \begin{cases} -1 \times (avg(Price) \times EV_{perform} \times d_{ij}) & , j \in s_j, a_i \in \{a_{r1}, a_{r2}\} \\ -1 \times [(avg\,(Price) \times EV_{perform} \times d_{ij}) + Price_{ch}(j)] & , j \in s_j, a_i \in \{a_{cr1}, a_{cr2}\} \\ -\infty & , j \notin s_j \end{cases} \tag{6}$$

$$Price_{ch}(j) = \sum_{t=t_{depa}(j)}^{t_{depa}(j)+t_{req}} (Price(t) \times P_{fast})/4 \tag{7}$$

TABLE 1. Result of reinforcement learning algorithm.

EVCS	-reward for charging cost per charging station
1	-1.2997
2	-1.3231
3	-1.3023
4	-1.3201
5	-1.3325
6	-1.3110
7	-1.3002
8	-1.3220

change. Therefore, assuming that the required charging time is charged at the electricity bill for that time based on the arrival time by the charging station, it can be expressed as (7), and the cost can be calculated. This is because SOC applied the initial SOC set for the vehicle and did not consider the energy used by the driving until it reached the charging station. The reason for dividing by 4 in the denominator is that we applied the time step to 15 minutes in this paper.

As a result of reinforcement learning in Table 1, after departure, it arrived at its destination through the charging station '3-5-2-8', and was charged at CS 3. The charging costs in Table 1 confirm that CS 3 is not the cheapest charging station. However, since the -reward for the distance was considered simultaneously, the same result can be obtained.

The cumulative -reward by the current driving route is -2.8138, and the cumulative -reward is -3.0614 when moving to 'departure-3-1-8-destination' in the case of charging at charging station 1. In the case of moving to 'Departure-3-1-8-7-Destination', it was not selected because the driving route was shorter even though there was a price difference of -3.0807. Therefore, among the optimal paths, charging is performed at charging station 3 because the charging cost of 3 is the cheapest among the charging prices of stations 2, 3, 5, and 8.

By the above equation, we design the driving scheduling of long-distance vehicles with reinforcement learning. We will explain the day-ahead scheduling algorithm for the EV aggregator of EV presented in this paper.

C. DAY-AHEAD SCHEDULING ALGORITHM FOR EV AGGREGATOR

Figure 8 shows the EV aggregator's day-ahead scheduling algorithm for the CS. The day-ahead scheduling algorithm aims to predict the EV driving schedule for the next day at the CS and plan the charging schedule accordingly. Therefore, the price is first delivered by the day-ahead time, and the CS performs EV driving schedule prediction. Based on the EV driving scheduling model described in section III above, the EV driving schedule prediction generates driving schedules for each vehicle with the number of EVs in the entire integrated system. The vehicle driving schedule data generated in this way is defined as one scenario, and in this paper, the

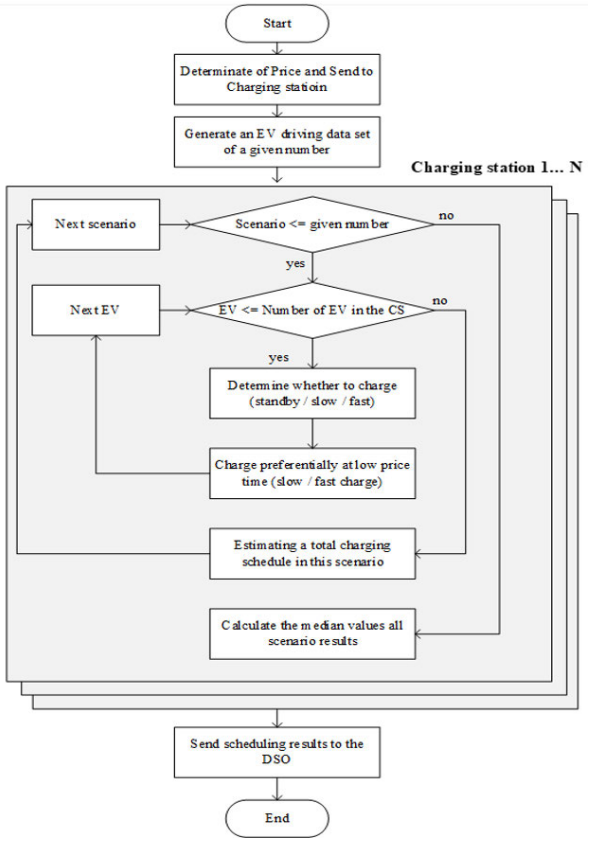

FIGURE 8. EV Aggregator's day-ahead scheduling algorithm flowchart.

charging schedule is set to derive based on 100 scenarios. After 100 EV driving schedules are created, it is determined whether each vehicle in one scenario is connected to a charging station.

Figure 9 shows a flowchart for these vehicle-specific charging schedules. In this figure, t_{st} is the time of the current entering vehicle, t_{b_st} is the time of previous entering vehicle at same charging station. Gamma distribution value is referred in equation (2), t_{req} is the time required to charge more than the required SOC, and $t_{parking}$ is the parking time. SOC can be divided into two types when entering the vehicle because the first entered vehicle will enter the vehicle with the SOC lowered through driving and because entering vehicles after more than one travel per day will be charged at the CS. In one scenario, all vehicles perform charging schedules in the same condition. When scheduling is performed for all vehicles connected to the daily CS, the same task is repeated for all scenarios. Subsequently, suppose the iterations are performed as many times as the set scenario. In that case, the median is calculated from the charging schedule of all scenarios and derived from the day-ahead charging scheduling. In the day-ahead charging scheduling algorithm, CSs derive scheduling results in a form that guarantees to charge schedules for individual EVs without any constraints. The charging time may be stagnant if the reservation results at the CS are confirmed throughout the system. Therefore, adjusting the charging demand of EVs in EV aggregators is necessary.

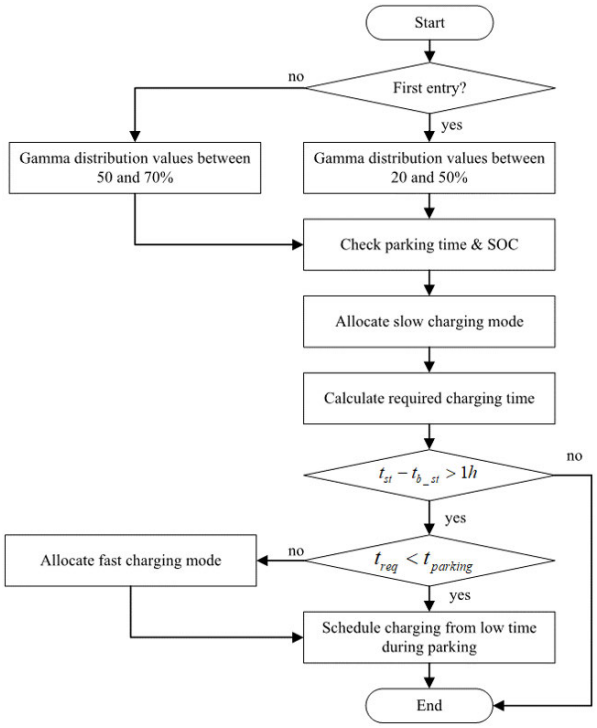

FIGURE 9. Charging schedule flowchart of each vehicle.

The cooperative scheduling algorithm in the EV aggregator is configured as a quadratic function, as shown in the formula below:

$$\min \sum_{t=T+1}^{T+4} \sum_{i \in AG} x_i(t)^2 + \omega x_j(t)^2 \tag{8}$$

$$\sum_{t=T+1}^{T+4} x_i(t) = \sum_{t=T+1}^{T+4} P_i^{\text{sch}}(t), \forall i \tag{9}$$

$$\sum_{i \in AG} (-1 \times x_i(t)) + x_j(t) = Load_j(t), \forall t \tag{10}$$

$$0 \le x_i(t) \le \max x_i(t), \forall t \tag{11}$$

$$\min f(x) \quad subject\ to: h(x) = 0; g(x) \le 0 \tag{12}$$

where i is the charging station, $x_i(t)$ is the charging station schedule by adjusted time, $x_j(t)$ is the general load for the entire system by adjusted time, AG is the number of charging stations in the system, T is the simulation time, $P_i^{\text{sch}}(t)$ is the submitted charging station schedule via time, $Load_j(t)$ is the general load for the entire system via time and ω is the weighting factor.

Equation (8) is an objective function for adjusting the charging schedule of the CS. The objective function is designed to find the minimum value of the sum of the square of the normal load and the square of the charging scheduling.

Equations (9)–(11) are constraints. Equation (9) requires the same amount of day-ahead scheduling power over an hour and the same amount of charging power after adjustment. Equation (12) is the formal expression of general ACOPF.

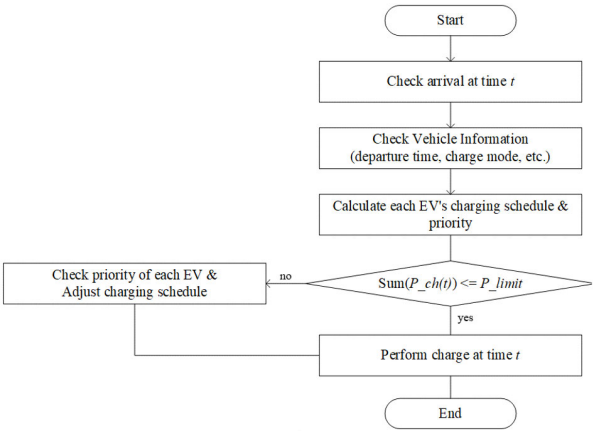

FIGURE 10. Charging station real-time charge control flowchart.

$f(x)$ means a control variable and a can be seen as an expression for power generation cost. An equivalent constraint, $h(x)$, is usually a constraint on the balance of active/reactive power. Non-equivalent constraints expressed by $g(x)$ include generator output limitations, line capacity limitations, and voltage ranges.

As previously mentioned, the EV driver chooses the charging time, which excludes EV aggregators from charging at different times, or at different prices. Therefore, this constraint allows shifting at a time step adjusted in 15-min intervals within the same time frame but prevents shifting to another time. In addition, as in the objective function, the algorithm is performed in hours, and the scheduling adjustment time is limited to one hour.

This is because when charging an electric vehicle, drivers generally prefer to charge it from a lower hour. The LMPs that EV drivers consider for the day-ahead charging schedule are announced hourly. Thus, scheduling can be adjusted within the same time frame, but EV drivers can make different choices at different prices so that scheduling can be adjusted simultaneously.

D. REAL-TIME CHARGING OF EV AGGREGATOR

Figure 10 shows a flowchart for real-time charging control. The flowchart in Figure 10 is made at every time step. Therefore, the CS checks whether the vehicle is parked at this time and checks information such as parking time and SOC. Subsequently, the charging schedule is carried out based on the data of each vehicle. For example, charging should be performed first in the case of fast charging, and charging should then be done considering the SOC for each vehicle, remaining parking time, and required charging time. After real-time charging scheduling, the priority of individual EVs is calculated. The formula for calculating priority is as follows:

$$PI_i(t) = \omega_1 pi_{soc}(i) + \omega_2 pi_t(i) + \omega_3 pi_{mode}(i) \tag{13}$$

$$\omega_1(i) = \frac{1 - e^{-\alpha \times SOC_i(t)}}{1 - e^{-\alpha(SOC_{req} - SOC_{min})}} \tag{14}$$

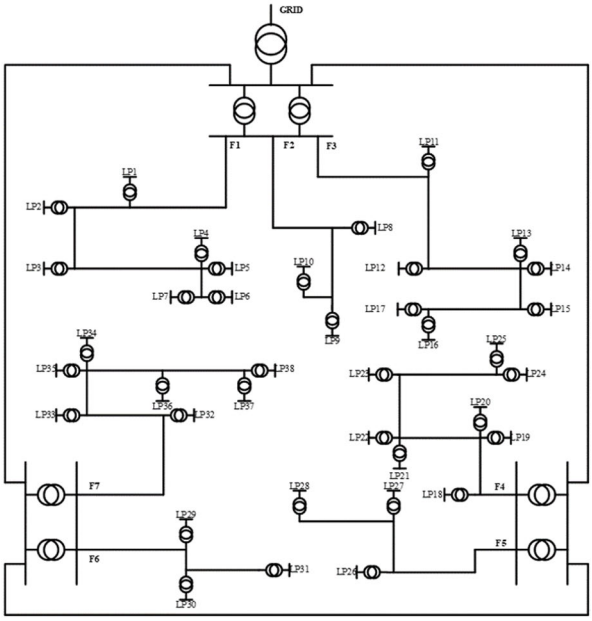

FIGURE 11. EV Aggregator's day-ahead scheduling algorithm flowchart.

$$\omega_2(i) = e^{-\beta \times \frac{PT_i(t) - t_{req}(t)}{PT_i(t)}} \tag{15}$$

$$\omega_3(i) = \begin{cases} 0, \textit{charging mode} = \textit{slow} \\ 1, \textit{charging mode} = \textit{fast} \end{cases} \tag{16}$$

where $PI_i(t)$ is the priority index of time t of vehicle i. $pi_{soc}(i)$, $pi_t(i)$ and $pi_{mode}(i)$ are the index of the required energy, charging time and charging mode of the vehicle i respectively. $PT_i(t)$ is the parking time of the vehicle i, α and β are the weight factor which set 5 and 10 respectively. Equation (13) is a calculation formula for the priority index for each vehicle, and Equations (14)-(16) are three weight calculation formulas. The priority index in Equation (13) is calculated as the sum of the products of each weight and the coefficient for each weight. At this time, $PI_i(t)$ appears as a value between 0 and 1. $PI_i(t)$ is set to 1 only for vehicles assumed to be long-distance traveling vehicles. This is because it was determined that, in the case of long-distance vehicles, charging at a low rate is important, but moving to a predetermined destination is important, so even if a situation in which the price fluctuates occurs, the choice is made to perform charging unconditionally.

IV. CASE STUDY

In this study, as shown in Figure 11, the power system modifies the IEEE RBTS Bus 4 system structure [27]. The system is selected because it has a radial distribution system structure, and the substation receiving power from the transmission system is implemented with six transformers and seven feeders, thereby making it suitable for plotting a small urban distribution system. The location and type of load were applied equally in the grid. In the IEEE RBTS system, only the average and peak loads are shown, so the case study applies the commercial and residential load patterns that fit with the same peak load. To add the EV charging station to this system, we extend the node so that the grid can transfer the energy to the charging system, as shown in Figure 11.

TABLE 2. Grid parameters.

Parameter	Value
Transformer Capacity	60 × 2 [MVA]
Branch Capacity	10 × 2 [MVA]
Reference Voltage	22.9 [kV]
Branch Impedance(r+jx)	0.0753 + j 0.136 [/km]

TABLE 3. Type and length of each branch.

Branch Type	Length [km]	Branch Number
1	1.8	1,3,4,8,12,15,17,20,23,26,27,28,32,35,46, 48,42,48,51,52,53,55,56,59,62,63,64,68,72, 75,78,81,82,85
2	2.25	2,6,9,11,14,19,24,29,31,34,40,43,47,50,54, 58,61,65,66,67,70,73,77,80,83
3	2.4	5,7,10,13,16,18,21,22,25,30,33,39, 44,45,46,49,57,60,69,71,74,76,79,84

TABLE 4. Load types and locations.

Load Points	Customer Type	Peak Load [MW]
1 − 4,11 − 13,18 − 21, 32 − 35	*Residential* 1	2.129
5,8,14 − 15,22 − 23,36 − 37	*Residential* 2	1.953
10,26 − 30	*Work* 1	3.912
9,31	*Work* 2	5.868
6 − 7,16 − 17,24 − 25,38	*Commercial*	1.611

TABLE 5. Electric vehicle charging feeder.

EVCS Number	Area	Feeder
1	Residential	1
2	Working	2
3	Residential	3
4	Residential	4
5	Commercial	4
6	Working	5
7	Working	6
8	Residential + Commercial	7

The main system parameters set by the simulated distribution system are defined in Table 2, track type and length as shown in Table 3, load type and location as shown in Table 4, and EVs charging feeder as shown in Table 5. This study assumes EVs have the same specifications, and simulations are performed by applying the parameters listed in Table 6. EV capacity and driving performance were applied to the Tesla Model S data [28]. At this time, the driving performance

TABLE 6. Electric vehicle and EV charger parameters.

Parameter	Value
Capacity [kWh]	62
Driving Performance [km/kWh]	2.775
Slow Charging Power [kW]	5
Fast Charging Power [kW]	50
SOC Range [%]	10–90
Target SOC (General) [%]	70
Target SOC (Long distance) [%]	90
Capacity [kWh]	62

is reduced to 50% performance to increase power usage, considering research convenience.

The number of EVs was calculated based on load peaks, and the number of vehicle registrations in California, United States, and 319.5 vehicles per MW was identified [29], [30]. The number of vehicles per MW at the peak was assumed according to the number of registered vehicles compared to the total load peak. Therefore, 2,706 EVs were set as the number of everyday EVs, assuming 10% of the total 27,052 EVs, and the number of long-distance EVs was set at 135 or approximately 5%.

In the entire integrated system, as previously described, the system operator submitted the forecast load to the higher system operator, and it was assumed that the LMP was calculated above and passed to the system operator. Therefore, it is assumed that the LMP is delivered in Figure 13, and the results of the subsequent steps are described. The general load of the entire grid is applied, as shown in Figure 12, and the following is the day-ahead charging load scheduling of the local EV aggregator. For day-ahead scheduling, the scheduling results are derived by applying the median value of the prediction scenario, as mentioned earlier.

Figure 14 shows the EVCS-specific day-ahead charging scheduling results based on the driving patterns of general EVs. The graph in blue on the figure shows the day-ahead scheduling result for each driving scenario, and the red is the day-ahead scheduling result submitted to the system operator. Figure 15 shows the scheduling results by EV aggregator for vehicles that perform fast charging over long distances. The charging station performs scheduling based on LMP, and most charging in the CS 1 region can be seen in Figure 15, and the charging time is also concentrated between 09:00 and 18:00 (Low-rate time). It was confirmed that some charging stations where charging schedules occur charge with base load during low price hours. As in the day-ahead scheduling results for everyday vehicles, it was inevitable that a large peak occurred for a short period of time right after the hourly price fluctuated. Therefore, to compensate for this problem, it is necessary to perform scheduling adjustment between charging stations.

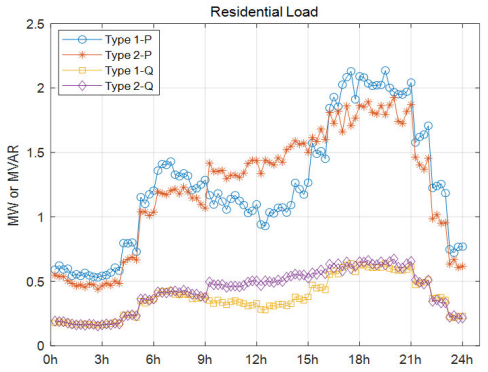

(a) Residential Load Profile

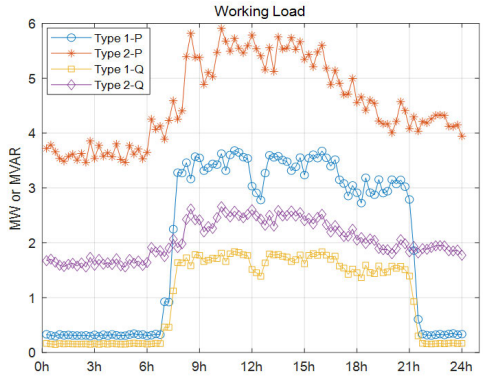

(b) Working Load Profile

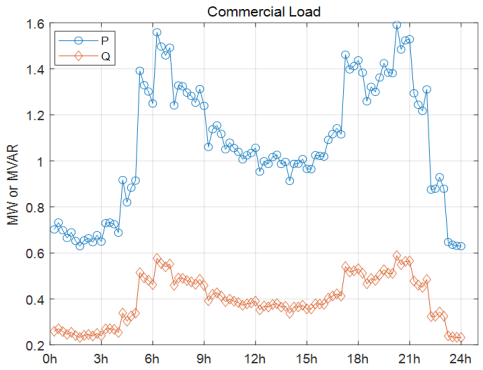

(c) Commercial Load Profile

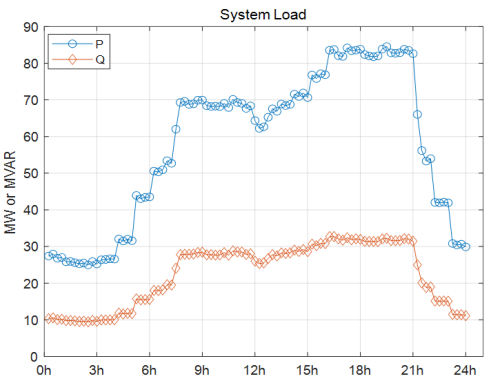

(d) Total System Load Profile

FIGURE 12. General load curve.

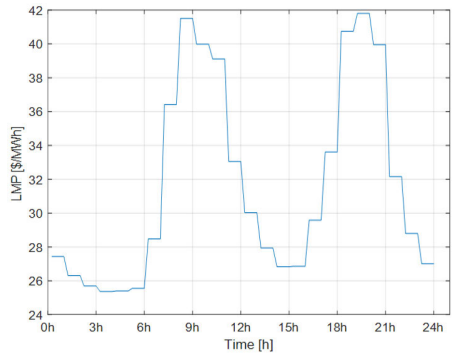

FIGURE 13. LMP profile.

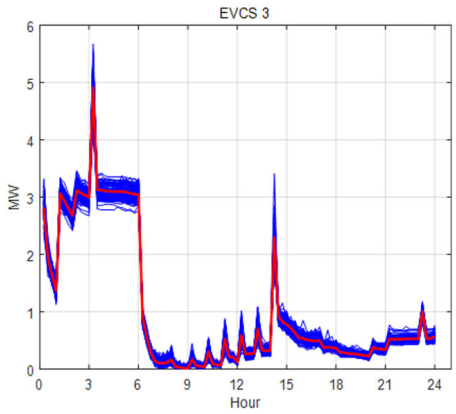

FIGURE 14. Day-ahead scheduling results of charging station (general vehicle).

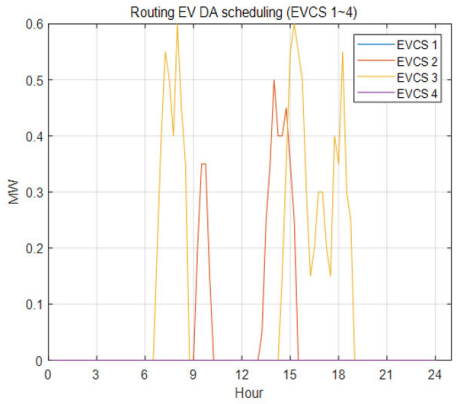

FIGURE 15. Day-ahead scheduling results of charging station (optimal path vehicle).

Figure 16 shows the day-ahead scheduling results of Figures 14 and 15. Although the number of optimal route-selecting vehicles in the system is only 5% compared to the usual vehicles in the system, it does not significantly affect overall scheduling; some CSs where the charging schedule occurs have been observed to charge the base load during low-cost times. It is inevitable that a large peak occurs for a short time immediately after the hourly price changes, such as in the results of day-ahead scheduling for routine vehicles.

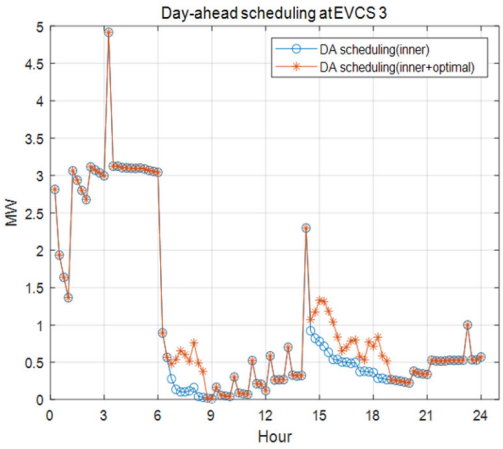

FIGURE 16. Day-ahead scheduling results of charging station.

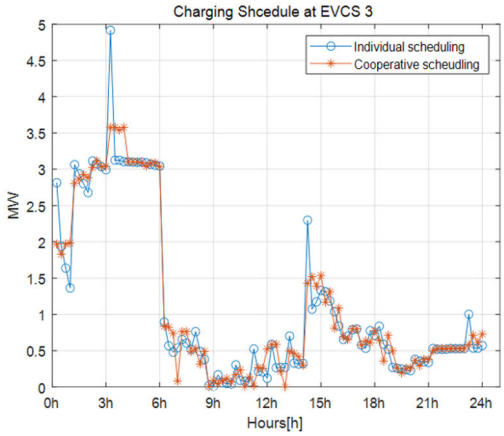

FIGURE 17. Comparison of EV CS's day-ahead scheduling results.

Therefore, performing scheduling adjustments between CSs to compensate for these problems is necessary.

Figure 17 shows the results of day-ahead scheduling and coordination scheduling of EVCS. As shown in the figure, it is confirmed that the load peak mitigated by scheduling adjustment is possible. Figure 17 shows that there is no significant difference from the existing scheduling in areas where the charging schedule is generally smooth, such as between 3 and 6 and 15 to 21; at 14:00, there is a significant effect of peak mitigation by scheduling adjustments.

In the coordinated scheduling, the charge load at that time remains at 1.5 MW on average, while the peak reaches a value of more than 4 MW in a moment. After the initial 15 min peak, the remaining 45 min were at 1 MW level, with considerable load fluctuations for an hour.

This can be seen as caused by EVs waiting for charging simultaneously as the LMP shows a low price during the afternoon from 14:00. Table 7 lists the parameters applied to the case study. This parameter contains the value of peak load, EV penetration rate, and the number of general and long distance EVs. During the charging schedule of EVs entering the day, the EVs charge at low-cost times depending

TABLE 7. Applied parameters.

Parameter	Value
Peak Load [MW]	84.54
Vehicle Penetration Rate [EV/MW]	320
EV Penetration Rate [%]	10
Number of EVs (general)	2,706
Number of EVs (long distance)	135

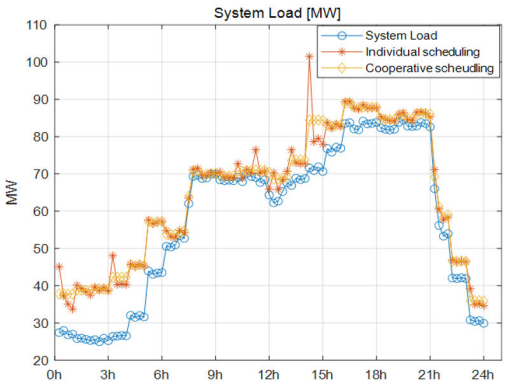

FIGURE 18. Comparison of EV charging schedule results with the day-ahead load.

on parking time, which is why charging power is concentrated in the early 14:00 when the price is low.

This can also be seen in EVCS peaks that occur significantly, and if these charging schedules are not controlled, they significant impact on the entire system, as shown in Figure 18. The peak that occurs at 14:00 exceeds 100 MW, which is more than 10 MW higher than the actual peak of approximately 90 MW at 16:00–17:00, significantly affecting the system's operation. Furthermore, compared to the general load peak, the existing peak load was approximately 84.5 MW, which increased to 88.5 MW, considering the charging demand of EVs. Thus, increasing peaks due to increasing loads due to EV charging are unavoidable. However, suppose the charging schedule is not adjusted in EV aggregators. In that case, unexpected peaks may occur in a non-peak time, or momentary peaks may lead to the need to expand facilities.

The following results from the DLMP calculations performed using MATPOWER [31]. Moreover, the facts observed in Figure 19 show that the cost had increased significantly since 18:00, when the existing load peaked.

The DLMP and LMP of EVCS with the highest values at the relatively low-load dawn time differ by \$0.6/MWh, but by peak time of 19:00, there is a \$2/MWh difference. In other words, the higher the load, the greater the overall system loss, indicating a more significant price difference. Figure 20(a) shows a price difference of approximately \$0.45/MWh at a significant reduction in the peak occurring suddenly.

Conversely, as shown in Figure 20(b), the DLMP increases at 15:00 when the load is increased by moving the lowered

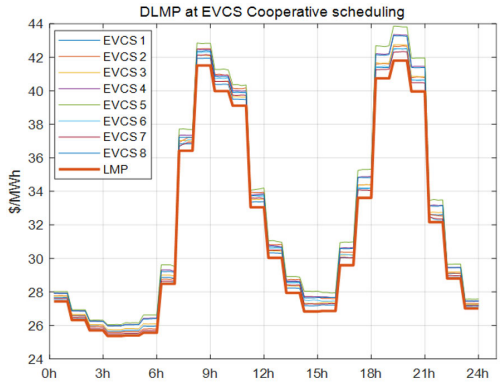

FIGURE 19. DLMP by adjustment scheduling.

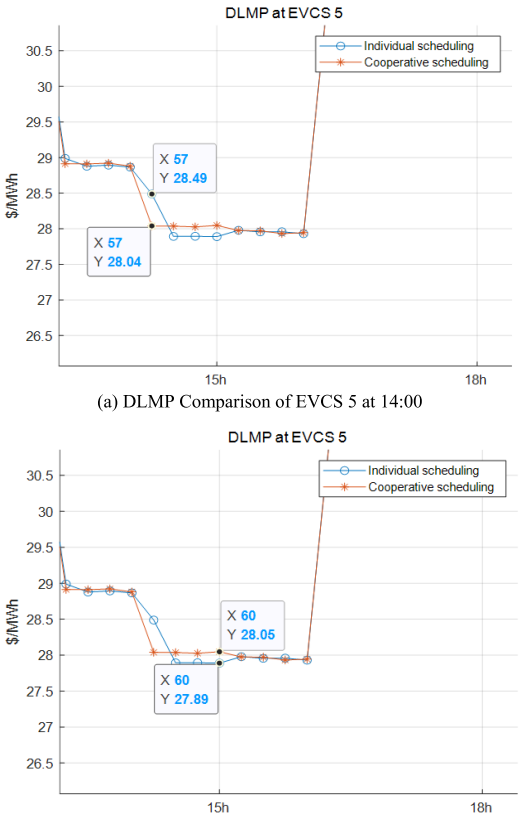

(a) DLMP Comparison of EVCS 5 at 14:00

(b) DLMP Comparison of EVCS 5 at 15:00

FIGURE 20. DLMP changes due to scheduling.

peak by the scheduling adjustment to that time. However, the price difference for this time is approximate \$0.16/MWh, resulting in a relatively smooth DLMP by scheduling adjustments. In Figure 20(a), which has the highest DLMP difference by scheduling adjustment, the price difference is only \$0.45/MWh; however, in proportion, the price reduction is 1.7%. There is a big difference in that this is not the result of shifting the price to another time but the price reduction that occurred simultaneously.

TABLE 8. Daily losses on integrated systems.

	Individual Scheduling	Cooperative Scheduling
Loss [MWh]	20.975	20.925

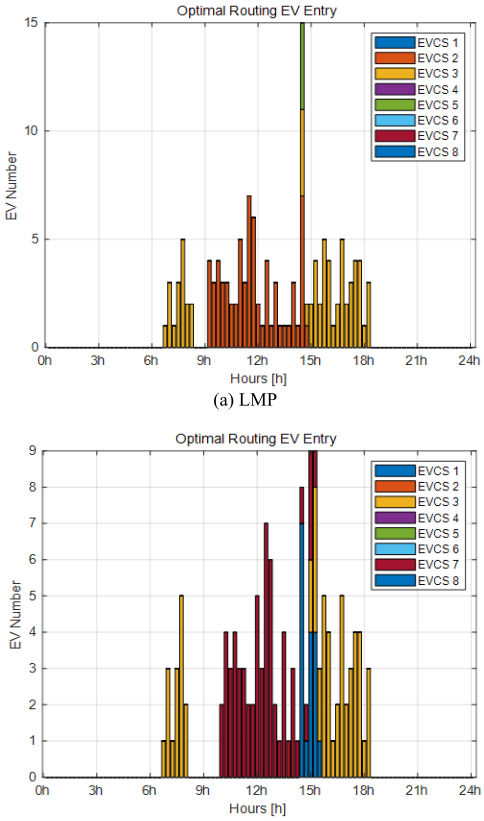

(a) LMP

(b) DLMP

FIGURE 21. EV number in real-time operation.

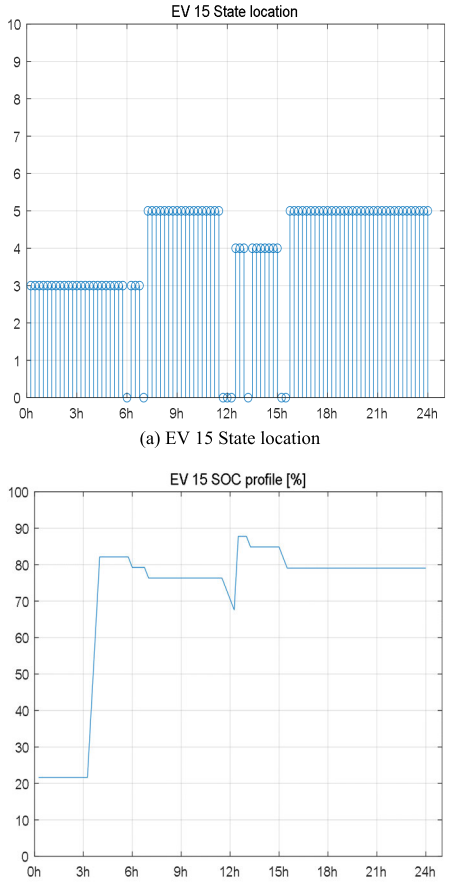

(a) EV 15 State location

(b) EV 15 SOC profile

FIGURE 22. Daily driving data of EV 15.

The cooperative operation algorithm between the EVCS adjusts the scheduling considering the EVCS and the loss of the overall system. It has been confirmed that the difference in DLMP is caused by the adjusted charging scheduling and maintaining the power system stability. Table 8 identifies a loss reduction of 0.05 MWh in daily losses. This is not a numerical significance level, but the total daily energy use is a loss reduction in the same situation.

The next step is to perform real-time operations after day-ahead scheduling. In real-time operation, the EV aggregator performs charging control based on the results of cooperative scheduling and selects the path by a specified LMP or DLMP. Figure 21 shows the time of entry for vehicles by optimal route selection. The vehicle arrives only during the daytime. This is because when modeling long-distance driving vehicles, the arrival time is set within the simulation time.

Therefore, vehicles that performed optimal route selection were aware of the DLMP determined the day-ahead, which could be considered when selecting the CS location. Based on the vehicle information entered, the peculiarity is that vehicles connected to EVCS 7 are more frequent than in other regions. This is because EVCS 7 has a low DLMP among EVCS except for LMP in Figure 19.

Furthermore, the EVCS-specific incoming vehicles show that they are concentrated in 1, 4, and 7, similar to EVCS 1, 4, and 7 located in the region closest to the departure-destination due to the structure of the transportation system. Compared to the EVCS-specific DLMP graph in Figure 18, fewer vehicles enter between 8 and 9 and 20 to 21 when the price is at its highest, which, as mentioned earlier, seems to charge before the price rises further or after a long time. Vehicles that make optimal route selection are charged with fast charging, which is performed for three-to-four-time steps. Therefore, if the vehicle is inspected between 11:00 and 12:00, many vehicles are arriving after 11:00 to 12:00, which is lower than before, when the price has risen further; vehicles entering EVCS 4 and 7 are charging in the nearest area to the destination where there is no place to charge, or in the nearest area before the price goes up further. EVCS 6 can be located nearby and similarly entered; however, as mentioned earlier, EVCS 6 is located at the end of the feeder and is not likely to be selected as higher prices are being formed.

Figure 22 (a) represents the data on the driving location. It is located in the EVCS 3 area from 0:00 to 6:00, and is connected to EVCS 3 again after driving for a while. Afterward, it moves to the EVCS 5 area again at 7:00, starts driving around 11:30, moves to the EVCS 4 area, parks for a while, drive again, and connects to EVCS 4. After that, it can be interpreted as driving just before 15:00 and arriving at EVCS 5. In addition, compared with Figure 22 (b), it can be seen that the battery is charged through rapid charging after 3:00 from the initial parking time. This is because the vehicle was pushed out of priority when charging with slow charging, and charging did not occur between 0:00 and 3:00, and after 3:00, the change to fast charging mode occurred due to low SOC and short charging time. Therefore, after the mode is changed, sufficient SOC has been secured through fast charging, and it can be confirmed that separate charging is not performed because it has sufficient SOC during the time zone connected to EVCS 5 for the first time.

As such, we checked the optimal route selection for EVs. However, in this case, revealing the objective of reducing system congestion and loss as targeted was difficult, as the difference in time changes by DLMP (up to \$0.45/MWh) is much more significant than the difference in price changes by DLMP.

V. CONCLUSION

In this study, we analyze the effect of charging EVs on the distribution grid with increasing EV penetration and experiment to control them through EV aggregators. The following structures and algorithms are proposed to analyze the impact of charging EVs on the system. To analyze the impact of charging EVs on the distribution system, a system with integrated transportation and power grids are designed. In the developed structure, the charging schedule is designed based on the driving schedule of the EV, and we design a structure to see that these charging loads also affect the power system. EV aggregators are designed in a hierarchical structure. This structure comprises EV aggregators in each region, performing full-day charging demand scheduling according to regional characteristics and coordinating day-ahead charging demand schedules at the top of EVCS that perform real-time charging control.

Developed integrated systems and development algorithms are constructed, and the charging demand of vehicles is achieved by modeling the EV driving schedule, charging schedule, and charging control of the EVCS. ACOPF is performed at a particular stage in the day-ahead to analyze the effect of charging EVs on the system, resulting in distributed LMPs. DLMP effectively determines the charging rate of EVs. At this time, if the system operator simply predicts the charging schedule of the vehicle and calculates and announces the DLMP, the DLMP at different times from the predicted charging demand can be lowered, thereby causing problems with the unexpected system. In this study, EV aggregators can contribute in terms of system stability to system operators by performing charge control based on predictive scheduling to compensate for these problems.

The study confirmed that the presence of EV aggregators could alleviate the peaks of integrated systems caused by the free charging of EV drivers and that the DLMP of the distribution grid could ease system congestion by moving vehicle movement and charging demand to other regions. The problem of peaks occurring during the initial period of price change at individual EV charging stations is resolved through the adjustment algorithm between EV aggregators. If the DSO can be coordinated with multiple EV aggregators in the distribution system, it can reduce the instantaneous peak in the grid and reduce the economic burden through the delay of power facilities. And as EV's charging patterns and charging location change depending on the price (DLMP), it can be seen as a demand response. In addition, EV drivers can charge at a lower rate, reducing the waiting time for charging. These findings can be used to simulate problems in the systems caused by increased EV distribution and to reflect them in the system operation and operation plan, as well as study the system operation method considering EVs with the presence of new market participants called EV aggregators. In the future, based on the integrated system developed in this paper, we plan to analyze the impact of LMP and power systems according to the timing of EV charging demand forecast in the LMP market model.

REFERENCES

[1] S. Shafiee, M. Fotuhi-Firuzabad, and M. Rastegar, "Investigating the impacts of plug-in hybrid electric vehicles on power distribution systems," *IEEE Trans. Smart Grid*, vol. 4, no. 3, pp. 1351–1360, Sep. 2013.

[2] IEA. (2019). *Global EV Outlook 2019*. [Online]. Available: https://www.iea.org/reports/global-ev-outlook-2019

[3] BloombergNEF. (2019). *Electric Vehicle Outlook*. [Online]. Available: https://about.bnef.com/electric-vehicle-outlook/#toc-viewreport

[4] *Main Contents and Implications of European EV Battery Promotion Policy*, Korea International Trade Association (KITA), Brussels, Belgium, Aug. 2019.

[5] Tesla. *Tesla Vehicle Safety Report*. Accessed: Aug. 8, 2022. [Online]. Available: https://www.tesla.com/VehicleSafetyReport

[6] L. McDonald. *Forcaset: US EV Sales Growth*, CleanTechnica. Jan. 20, 2019. [Online]. Available: https://cleantechnica.com/2019/01/20/forecast-2019-us-ev-sales-growth-will-drop-to-12/

[7] M. Etezadi-Amoli, K. Choma, and J. Stefani, "Rapid-charge electric-vehicle stations," *IEEE Trans. Power Del.*, vol. 25, no. 3, pp. 1883–1887, Jul. 2010.

[8] S. Faddel and O. Mohammed, "Automated distributed electric vehicle controller for residential demand side management," in *Proc. IEEE Ind. Appl. Soc. Annu. Meeting*, Cincinnati, OH, USA, Oct. 2017, pp. 1–8.

[9] P. Y. Kong and G. K. Karagiannidis, "Charging schemes for plug-in hybrid electric vehicles in smart grid: A survey," *IEEE Access*, vol. 4, pp. 6846–6875, 2016.

[10] S. I. Vagropoulos, D. K. Kyriazidis, and A. G. Bakirtzis, "Real-time charging management framework for electric vehicle aggregators in a market environment," *IEEE Trans. Smart Grid*, vol. 7, no. 2, pp. 948–957, Mar. 2016.

[11] A. Gholami, T. Shekari, F. Aminifar, and M. Shahidehpour, "Microgrid scheduling with uncertainty: The quest for resilience," *IEEE Trans. Smart Grid*, vol. 7, no. 6, pp. 2849–2858, Nov. 2016.

[12] G. R. Bharati and S. Paudyal, "Coordinated control of distribution grid and electric vehicle loads," *Electr. Power Syst. Res.*, vol. 140, pp. 761–768, Nov. 2016.

[13] Q. Zhang, Y. Hu, W. Tan, C. Li, and Z. Ding, "Dynamic time-of-use pricing strategy for electric vehicle charging considering user satisfaction degree," *Appl. Sci.*, vol. 10, p. 3247, May 2020.
[14] H.-J. Lee, H.-J. Cha, and D. Won, "Economic routing of electric vehicles using dynamic pricing in consideration of system voltage," *Appl. Sci.*, vol. 9, no. 20, p. 4337, Oct. 2019.
[15] L. Bai, J. Wang, C. Wang, C. Chen, and F. Li, "Distribution locational marginal pricing (DLMP) for congestion management and voltage support," *IEEE Trans. Power Syst.*, vol. 33, no. 4, pp. 4061–4073, Jul. 2018.
[16] R. Li, Q. Wu, and S. S. Oren, "Distribution locational marginal pricing for optimal electric vehicle charging management," *IEEE Trans. Power Syst.*, vol. 29, no. 1, pp. 203–211, Jan. 2014.
[17] X. Shi, Y. Xu, Q. Guo, H. Sun, and W. Gu, "A distributed EV navigation strategy considering the interaction between power system and traffic network," *IEEE Trans. Smart Grid*, vol. 11, no. 4, pp. 3545–3557, Jul. 2020.
[18] M. Amini and O. Karabasoglu, "Optimal operation of interdependent power systems and electrified transportation networks," *Energies*, vol. 11, no. 1, p. 196, Jan. 2018.
[19] B. Ferguson, V. Nagaraj, E. C. Kara, and M. Alizadeh, "Optimal planning of workplace electric vehicle charging infrastructure with smart charging opportunities," in *Proc. 21st Int. Conf. Intell. Transp. Syst. (ITSC)*, Nov. 2018.
[20] N. Z. Xu, K. W. Chan, C. Y. Chung, and M. Niu, "Enhancing adequacy of isolated systems with electric vehicle-based emergency strategy," *IEEE Trans. Intell. Transp. Syst.*, vol. 21, no. 8, pp. 3469–3475, Aug. 2020.
[21] P. Prabawa and D.-H. Choi, "Multi-agent framework for service restoration in distribution systems with distributed generators and static/mobile energy storage systems," *IEEE Access*, vol. 8, pp. 51736–51752, 2020.
[22] Z. Ye, C. Chen, B. Chen, and K. Wu, "Resilient service restoration for unbalanced distribution systems with distributed energy resources by leveraging mobile generators," *IEEE Trans. Ind. Informat.*, vol. 17, no. 2, pp. 1386–1396, Feb. 2021.
[23] Z. Wei, Y. Li, and L. Cai, "Electric vehicle charging scheme for a park-and-charge system considering battery degradation costs," *IEEE Trans. Intell. Vehicles*, vol. 3, no. 3, pp. 361–373, Sep. 2018.
[24] A. Dogan and M. Alci, "Heuristic optimization of EV charging schedule considering battery degradation cost," *Elektronika Elektrotechnika*, vol. 24, no. 6, pp. 15–20, Dec. 2018.
[25] Y. Wang and D. Infield, "Markov chain Monte Carlo simulation of electric vehicle use for network integration studies," *Int. J. Elect. Power Energy Syst.*, vol. 99, pp. 85–94, Jul. 2018.
[26] M. Alizadeh, H.-T. Wai, M. Chowdhury, A. Goldsmith, A. Scaglione, and T. Javidi, "Optimal pricing to manage electric vehicles in coupled power and transportation networks," *IEEE Trans. Control Netw. Syst.*, vol. 4, no. 4, pp. 863–875, Dec. 2017.
[27] R. Billinton, S. Kumar, N. Chowdhury, K. Chu, K. Debnath, L. Goel, E. Khan, P. Kos, G. Nourbakhsh, and J. Oteng-Adjei, "A reliability test system for educational purposes-basic data," *IEEE Power Eng. Rev.*, vol. 9, no. 8, pp. 67–68, Aug. 1989.
[28] F. Lambert, "Tesla discontinues model 3 mid range battery pack," Electrek, Fremont, CA, USA, Tech. Rep., Mar. 2019.
[29] CAISO. *California ISO Peak Load History 1998 Through 2019*. Accessed: Feb. 14, 2021. [Online]. Available: https://www.caiso.com/Documents/CaliforniaISOPeakLoadHistory.pdf
[30] Statista. *Number of Registered Automobiles in California 2018*. [Online]. Available: https://www.statista.com/statistics/196024/number-of-registered-automobiles-in-california/
[31] R. D. Zimmerman, C. E. Murillo-Sanchez. (2019). *MATPOWER (Version 7.0)*. [Online]. Available: https://matpower.org

HEEJUNE CHA was born in Chuncheon, Republic of Korea, in 1990. He received the B.S., M.S., and Ph.D. degrees in electrical engineering from Inha University, Incheon, South Korea, in 2013, 2015, and 2020, respectively. He is currently a Senior Researcher with Incheon International Airport Corporation (IIAC), Incheon. His research interests include distribution system operation, energy storage systems, and electric vehicle.

MYEONGSEOK CHAE (Student Member, IEEE) was born in Incheon, Republic of Korea, in 1998. He received the B.S. degree in electrical engineering from Inha University, Incheon, in 2021, where he is currently pursuing the M.S. degree in electrical engineering. His research interests include microgrids, distributed energy resources, and energy storage systems.

MUHAMMAD AHSAN ZAMEE was born in Dhaka, Bangladesh, in 1987. He received the B.Sc. degree in electrical, electronic, and communication engineering from the Military Institute of Science and Technology, Dhaka, in 2009, the M.Sc. degree in electrical and electronic engineering from the Islamic University of Technology, Gazipur, Bangladesh, in 2015, and the Ph.D. degree in electrical and computer engineering from Inha University, Incheon, South Korea, in 2020. He is currently a Postdoctoral Fellow with the Inha Power System Laboratory, Inha University. His research interests include the application of artificial intelligence and nature-inspired optimizations in power and control systems.

DONGJUN WON (Member, IEEE) received the B.S., M.S., and Ph.D. degrees in electrical engineering from Seoul National University, Seoul, South Korea, in 1998, 2000, and 2004, respectively. He was a Postdoctoral Fellow with the APT Center, University of Washington, Seattle. Currently, he is a Professor with the School of Electrical Engineering, Inha University, Incheon, South Korea. His research interests include power quality, microgrids, renewable energy, electric vehicle, and energy storage systems.